# PROBLEMS WITH RESISTIVE PASTE PREPARATION

## Invited Paper, SD-91 Conference, Portorož

R. Kužel, I. Křivka, O. Stefan, J. Kubát, M. Hrovat, D. Rafaja, J. Pešička, J. Prokeš, J. Broukal

**KEYWORDS:** resistive paste, glass powder, $RuO_2$ powder, thick film resistors, thick film technology, materials properties, grain size, percolation, blending curves, temperature coefficient of resistance, voltage dependence of resistance, electrical resistance, microscopy, X-ray analysis, experimental results

**ABSTRACT:** There are several problems connected with resistor paste preparation: the selection of a suitable glass frit and electrical conductive solid ingredients, namely $RuO_2$. Several types of $RuO_2$ powders prepared by various producers were tested using X-ray analysis and microscopy methods. The lattice parameters, microstrain and grain sizes were determined by these experiments. Our new tested pastes were prepared with microcrystalline $RuO_2$ powder (by Shoei Chemical Inc.) and resistive thick films were measured (resistivity dependence on $RuO_2$ contents, temperature dependence of resistance, temperature coefficient of resistance etc.). It was shown that the percolation theory was suitable for the explanation of some results obtained.

# PROBLEMI PRI PRIPRAVI UPOROVNIH PASTI

## Uvodno predavanje SD-91, Portorož

**KLJUČNE BESEDE:** uporovne paste, steklen prah, $RuO_2$ prah, debeloplastni upori, tehnologija debelih plasti, lastnosti materiala, velikost zrn, perkolacija, krivulje mešanja, temperaturni koeficient upornosti, napetostna odvisnost upornosti, električna upornost, mikroskopija, rentgenska analjiza, eksperimentalni rezultati

**POVZETEK:** S pripravo uporovnih plasti je povezanih kopica problemov: izbira ustreznih kalciniranih zmesi in električno prevodnih trdnih sestavin, kot je npr. $RuO_2$. Več vrst $RuO_2$ prahu pripravljenega na različne načine smo testirali z uporabo x-žarkovne analize in mikroskopskih metod. Kristalni parametri, mikronapetosti in velikost zrn smo določili s pomočjo omenjenih eksperimentov. Naše nove uporovne paste smo pripravili iz mikrokristaliničnega $RuO_2$ prahu (proizvajalec Shoei Chemical Inc.) ter opravili meritve uporovnih debelih plasti (odvisnost upornosti od vsebnosti $RuO_2$, temperaturno odvisnost upornosti, temperaturni koeficient upornosti itd.). Pokazali smo, da s perkolacijsko teorijo lahko ustrezno obrazložimo nekatere dobljene rezultate.

## 1. INTRODUCTION

Resistor pastes are very important components for hybrid circuits. We would like to devote ourselves to complex problematics of resistive pastes and resistor preparation.

Deciding to solve this task, we must be prepared to have to solve a lot of problems in order to obtain the pastes with reproducible and required properties of produced thick film resistors. This concerns a choice of precursor materials, technology equipments and measurement set-up used for diagnostics of every interproduct after individual process step.

For several years we have been successful in bringing together several small working teams from various institutes and forming an informal common laboratory for the solution of these problematics. You may ask, why engage ourselves in these problems when a lot of producers have already solved the tehnology of resistive pastes and offer their various types. We can name the following producers: Du Pont, Remex, Electro-Science Laboratories, Inc., Shoei Chemical Inc. etc. However, we know these producers carry out an intensive investigation of new pastes with better properties. The latest results of the last research work were presented by research engineer N. Yoshida of Shoei Chem. Inc. in the paper (1) entitled "50 ppm Thick Film Resistors in Relation with Pattern Size and Termination Materials" at the ISHM' 91European Hybrid Microelęctronics Conference, held in Rotterdam in 1991.

The second reason is that we wanted to study the physics and physical properties as well as processes connected with resistive thick films. The third reason is to prepare own resistive pastes with required properties at the cost as low as possible.

We are going to take up individual problems in detail in the following chapters.

## 2. RESISTOR PASTE PREPARATION

Resistor pastes consist of three basic components which are principal and must be solved. They are as follows: glass frit, electrical conductive solid ingredients and a liquid vehicle.

### 2.1. Glass frit and glass powder

To find the best glass frit is a very difficult problem as there are lots of possibilities how to prepare the glass. Components of glass can vary considerably both as to the used compounds (namely oxides) and to their amounts. The following compounds are mostly used: PbO, $B_2O_3$, $Bi_2O_3$, $SiO_2$, BaO, ZnO, $ZrO_2$, $Al_2O_3$, CaO, CoO etc.

Glass frit preparation:

The first step: pelletizing glass components at 350°C - 450°C for about 60 minutes.

The second step: melting pelletized glass components in a suitable platinum-rhodium crucible weighing up to 50 kilograms at 1250 - 1450°C with intensive mixing for about 60 minutes.

The third step: fritting melted glass into destilled water or between two water - cooled rotating cylinders.

### Glass powder preparation;

Glass powder can be prepared using any approapriate grinding mill, for example a planetary ball grinding mill Fritsch Pulverisette 5 with a suitable garniture (agate, alumina, tungsten carbide etc.) Grinding takes about 20-50 hours depending on the glass type. When no powder abrasion is necessary, a jet mill can be used (for example type Labor TX by Bauermann).

The amount of prepared ground powder ranges from 0.5 to 5 kilograms per hour. The particle sizes are mostly less than 3 μm.

### 2.2 Electrical conductive ingredients

Ruthenium compounds are chosen usually as the main electrically conductive solid ingredients used for resistive paste preparation as follows: $Pb_2Ru_2O_6$, $Bi_2Ru_2O_7$, $RuO_2$.

The resistive pastes developed in the last years contain first of all ruthenium dioxide. That is why we also tried to prepare some pastes based on this compound. Ruthenium dioxide is being produced and sold by several firms as follows: Engelhard, Degussa, Johnson-Matthey, Shoei Chemical Inc. etc.

When we bought $RuO_2$ from these producers, we found that structure and particle sizes of powders were quite different.

We tried to prepare $RuO_2$ also by ourselves. The microscopy investigations and X-ray analyses of ruthenium dioxide of different kinds are described in the following chapters.

### 2.3. Paste mixing

A paste can be prepared by mixing components as such glass frit and conductive ingredients and a suitable liquid vehicle. Terpineol or butyl carbitol solvent with 10 wt.% ethyl cellulose can be used as the liquid vehicle. For small amounts of the paste a suitable grinding equipment can be used, for example Pulverisette 2 by Fritsch. An equipment with two rotating stainless cylinders is suitable for great volumes of the paste.

## 3. GLASS, GLASS POWDER AND PASTE TESTING

In order to obtain reproducible pastes, all their components have to be properly tested.

We determine the following data and parameters for the glass frits:

- density
- thermal expansion coefficient,
- transformation point Tg,
- deformation point Td,
- sealing temperature Ts,
- glass composition and additives (by means of electron microprobe usually).

After glass grinding, we are interested in a quality of finely ground powder and investigate particle size distribution and surface area (in $m^2/g$) by means of suitable equipment (for example produced by Micromeritics: Sedigraph 5100 and Asap 2000, respectively).

The reproducibility of fired thick films (their thickness) is also determined by paste viscosity. It can be measured by a suitable viscometer. The viscometers produced by Brookfield are used very often.

(Note: Any glass frit and glass powder can be prepared and tested in the State Glass research Institute in Hradec Kralové.)

## 4. MICROSCOPY INVESTIGATION OF $RuO_2$ POWDERS

The microscopy investigation, especially transmission electron microscopy using microscopes Jeol FX 2000 and Tesla ES 540, was chosen for testing the $RuO_2$ powders prepared by various methods and offered by the above mentioned well-know producers. The forms and sizes of individual grains and clusters were observed in microscopes when using dark or light field methods and electron diffraction.

This investigation showed the results as follows:

1) The $RuO_2$ powder of Engelhard production formed polycrystal clusters (see Fig. 1a) containing very small grains as proved by electron diffraction pattern (see Fig. 1b).

2) The similar results were obtained by investigation of Johnson-Matthey $RuO_2$ powder, type 800-2MX, (see Fig. 2a). Only particle sizes were smaller than those in the Engelhard powder as Fig. 2b demonstrates.

3) Much biger single crystal grains were observed in the second Johnson-Matthey powder, type 800-3C. Figure 3a shows individual single crystals with shapes closed to spheres. The electron diffraction pattern ( see Fig. 3b) confirmed larger sizes of grains.

4) Very interesting micrographs were from $RuO_2$ powder, type Ru-109, produced by Shoel Chemical Inc. The individual grains were formed by perfectly created single crystals. They were of a regular tetragonal structure with sizes about 50x34 nm (see Fig. 4a). The crystal faces were very well developed and we can assume their high stability and resistance to the surrounding medium. The electron diffraction pattern (Fig. 4b) shows that particle sizes are somewhat smaller than those of Johnson-Matthey powder (800-3C). A considerable priority of this powder is the fact that grains do not form conglomerates and clusters as demonstrated also by a micrograph made by Tesla microscope (see Fig. 5).

5) We tried to prepare ruthenium dioxide which would be suitable for the resistive paste preparation using several tehnology methods.

The first method consisted in ruthenium oxidation at 1.200°C with subsequent grinding in a planetary agate mill. The $RuO_2$ powders contained various grains ranging from about several nanometers up to 300 nm. The grains were represented by single crystals, as we can see in Fig. 6. It was difficult to prepare smaller and uniform particles for the resistor paste preparation by this method.

The second method using heat treatment of $RuCl_3$ at 500°C for 5 hours was not suitable either. The $RuO_2$ grains, shown in Fig. 7, were quite irregular and mostly formed by oblong and sharp particles, their lengths were about 200 - 800 nm.

After quite a considerable effort, we were successful in obtaining the powder represented by small single crystalline grains, long about 25 nm (see Fig. 8), with well developed faces and squared bases. The electron diffraction pattern confirmed small single crystals. The properties and suitability of this powder for resistor paste preparation have been still under investigation.

The obtained results showed the variety of different $RuO_2$ powders which caused various values of sheet resistence and temperature coefficient of resistance of thick film resistors, when using the pastes containing these powders (2).

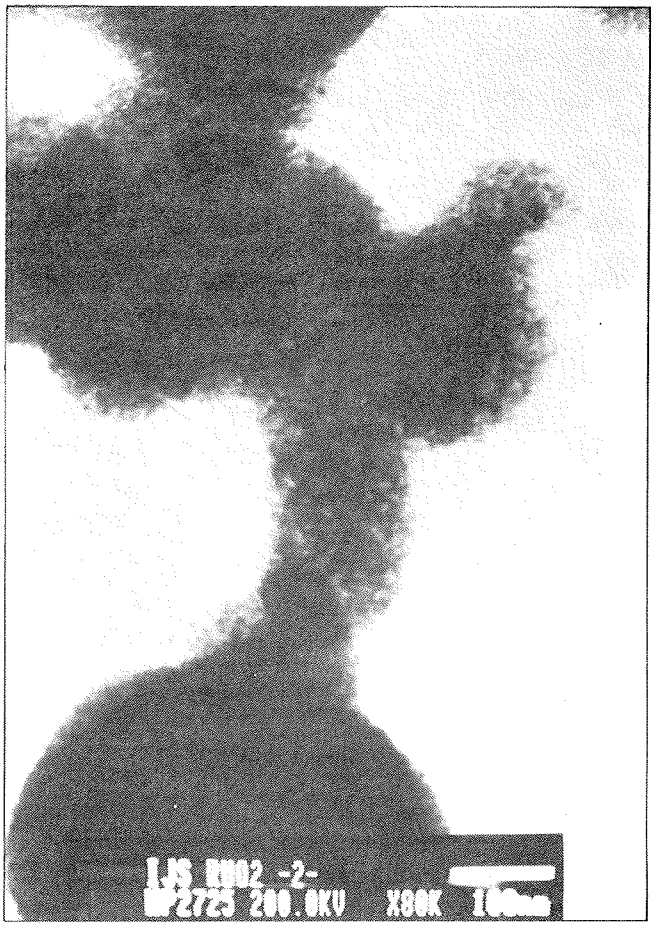

*Fig. 1a: Micrograph of $RuO_2$ powder (by Engelhard).*

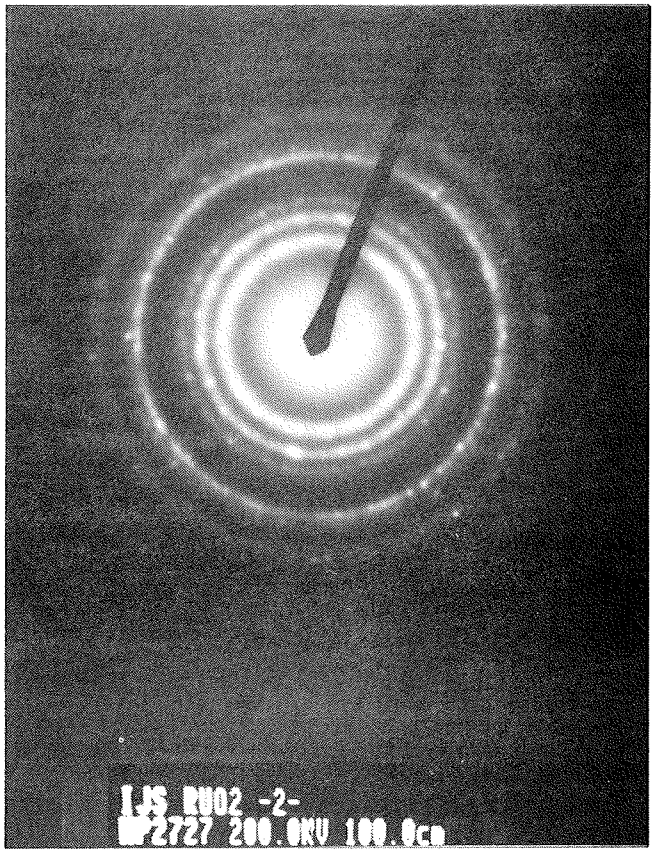

*Fig. 1b: Electron diffraction pattern from $RuO_2$ powder (by Engelhard).*

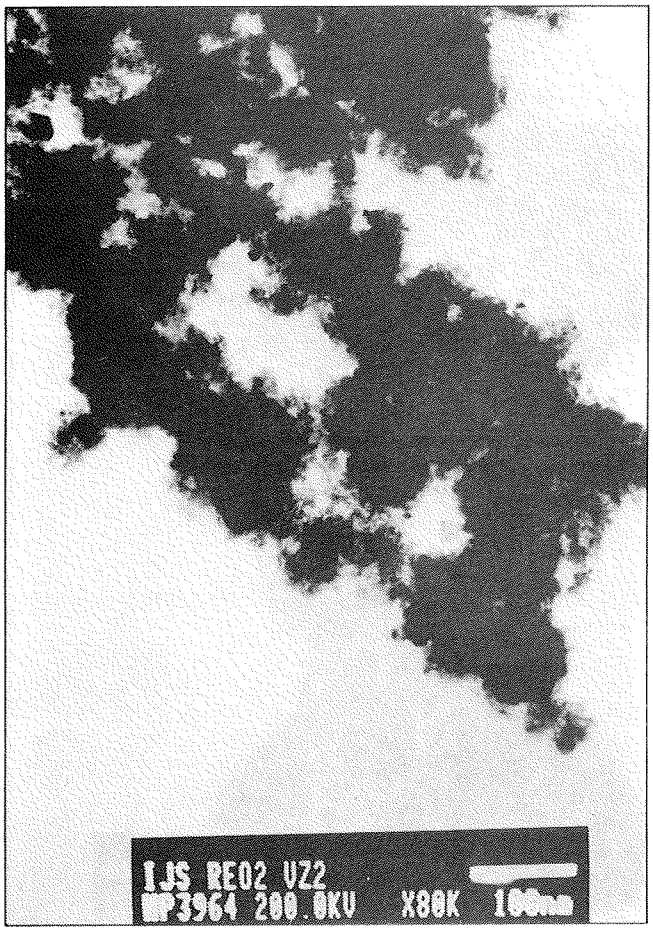


Fig. 2a Micrograph of $RuO_2$ powder (type 800-2MX by Johnson-Matthey).

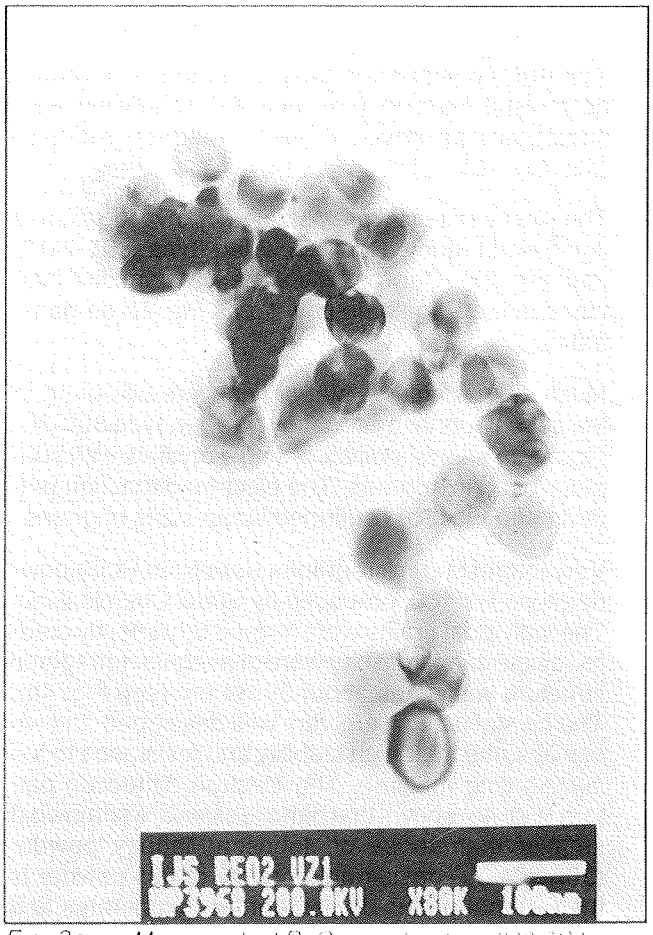


Fig. 3a. Micrograph of $RuO_2$ powder (type 800-3C by Johnson-Matthey).

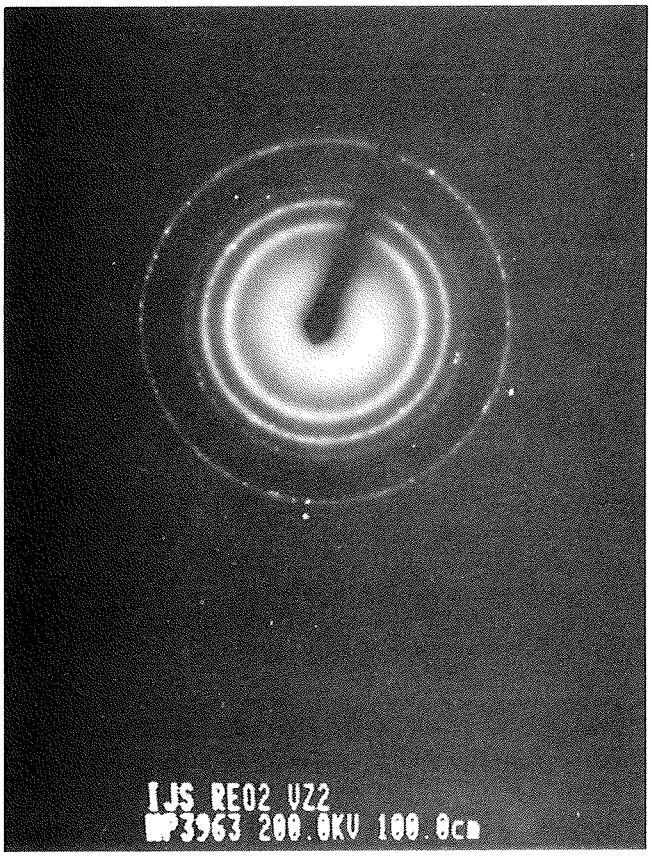


Fig. 2b: Electron diffraction pattern from $RuO_2$ powder (type 800-2MX by Johnson-Matthey).

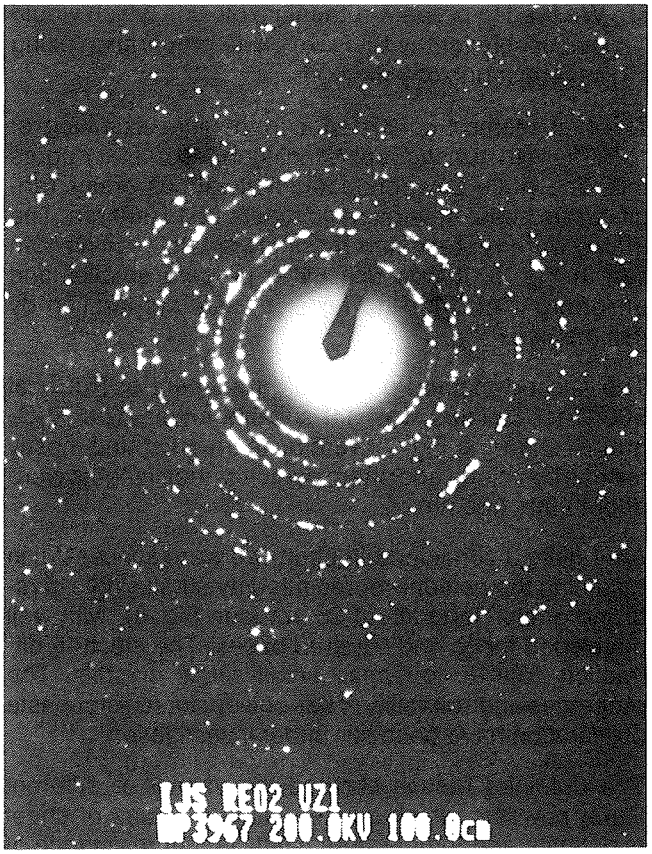


Fig. 3b: Electron diffraction pattern from $RuO_2$ powder (type 800-3C by Johnson-Matthey).

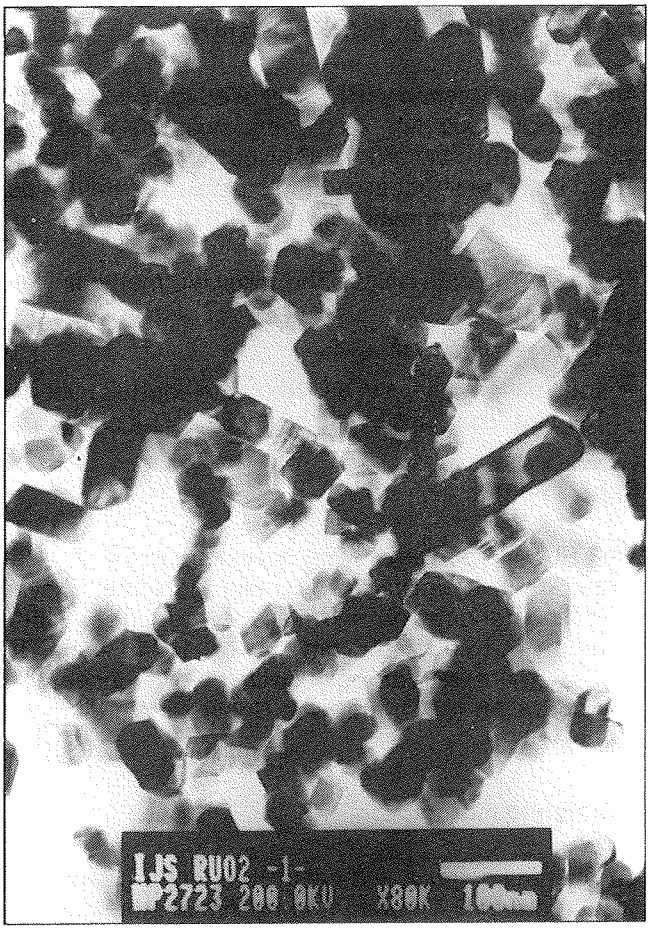


Fig. 4a. Micrograph of $RuO_2$ powder (type Ru-109 by Shoei Chem. Inc.).

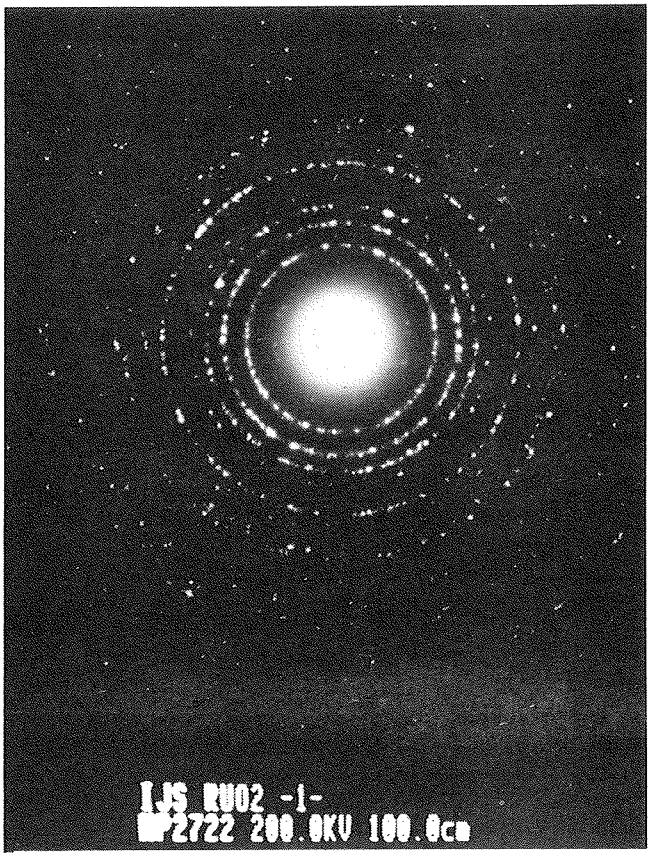


Fig. 4b: Electron diffraction pattern from $RuO_2$ powder (type Ru-109 by Shoe Chem. Inc.).


Fig. 5: Micrograph of $RuO_2$ powder of type Ru-109 shows perfectly created microrystalline grains without clusters and conglomerates.

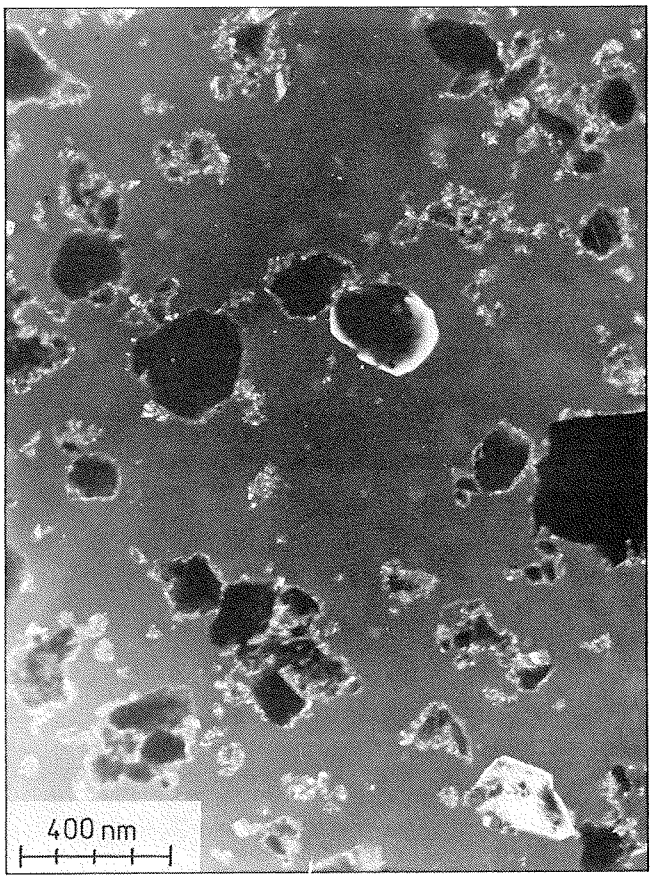


Fig. 6: Micrograph of $RuO_2$ powder prepared by ruthenium oxidation at 1,000°C (ground for 40 hours).

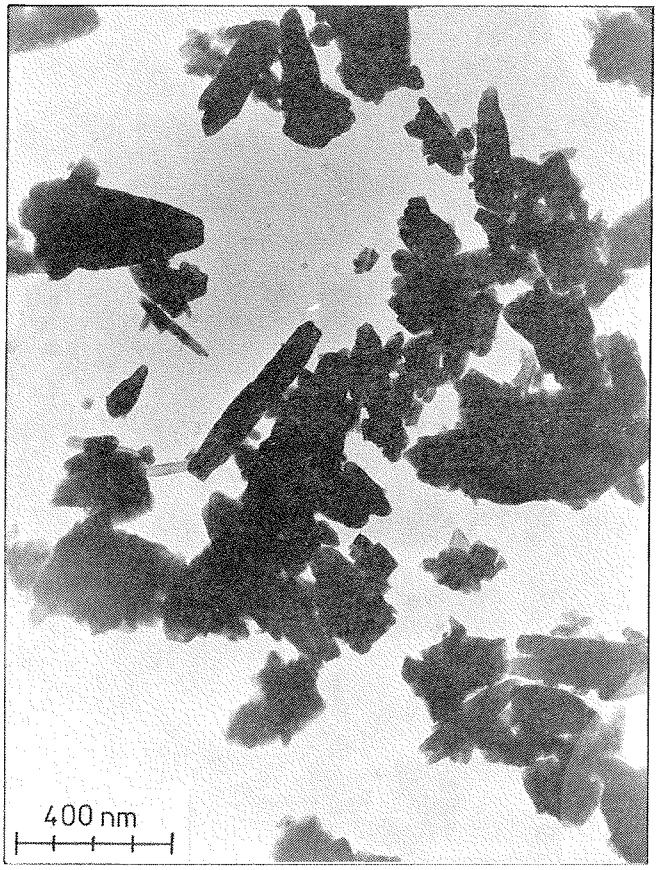


*Fig. 7: Micrograph of $RuO_2$ powder prepared by heat treatment of $RuCl_3$ at 500°C.*

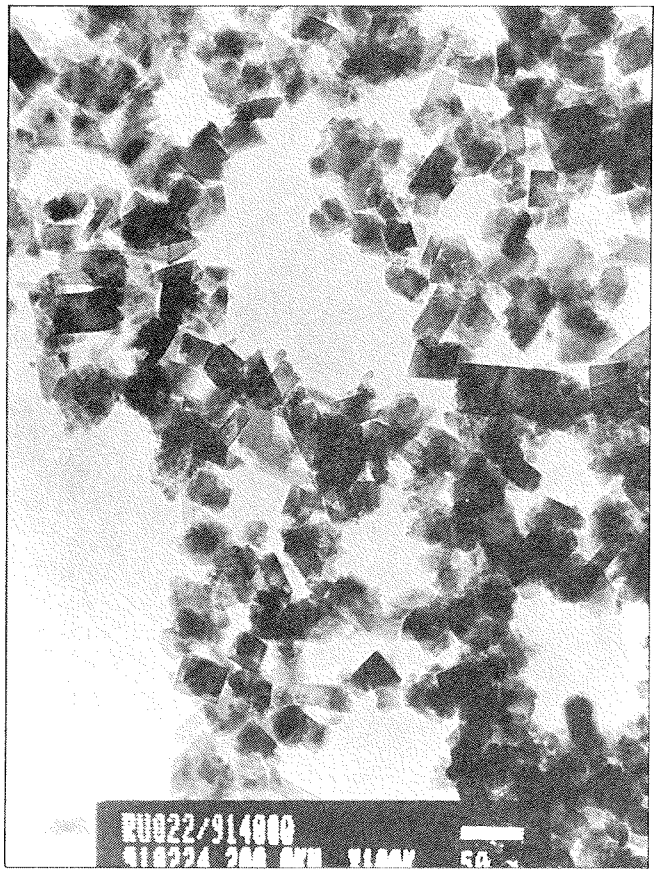

*Fig. 8: Micrograph of $RuO_2$ powder prepared by our methods.*

## 5.X-RAY STUDY OF $RuO_2$ POWDERS

An X - ray diffraction (XRD) was used for the investigation of $RuO_2$ powders as a complementary method to the electron microscopy. XRD gives the total information about both the structure and microstructure (lattice parameters, grain (domain) size, strain) of samples.

For the X-ray data anlysis the following methods were used:

- Rietveld pattern analysis,
- total pattern analysis based on the approximation of measured profiles by some analytical functions.

### Experimental

The $RuO_2$ - powerds were investigated by X - ray diffraction using a Bragg - Brentano goniometer (symmetrical arrangement) and a monochromatized CuKα radiation ($\lambda_1$ = 0.15405 nm, $\lambda_2$ = 0.15445 nm). The measurement was carried out with the divergence slit in primary beam ($\delta$=1°) and with Soller slits in diffracted beam.

### Evaluating methods

Lattice parameters a and c of the tetragonal cell of $RuO_2$ (space group P $4_2$/mnm) and fractional atomic coordinates of oxygen were determined using the Rietveld analysis (3).

*Fig. 9: Electron diffraction pattern from $RuO_2$ powder prepared by our method.*

Both the grain size (coherent domain size) D and the strain e (inhomogeneous relative change of lattice spacing) can be determined from line broadening, but the integral breadths must be corrected for an instrumental influence. If both, the total experimental profile and instrumental broadening are Cauchy functions, then the linear relation

$$B^f = B^h - B^g \quad (1)$$

is valid, where the indices f, h and g indicate the physical, measured and instrumental broadenings, respectively (4). It can be written (4):

$$B^f(hkl) = 1/D + (4e/\lambda) \sin \Theta_{hkl}, \quad (2)$$

where $\Theta_{hkl}$ denotes the Bragg angle of reflection hkl.

As the dependence of the integral breadths on the direction (hkl) was observed, the Rietveld analysis cannot be used for investigation of these parameters. Therefore, the experimental data were fitted using a more precise total pattern analysis, (see (5)).

## Results

Rietveld analysis of the whole diffraction profile (for powder of $RuO_2$, type Ru-109) is shown in Figure 10. The most important structure parameters and their errors as determined by using the Rietveld pattern analysis are given in Table 1.

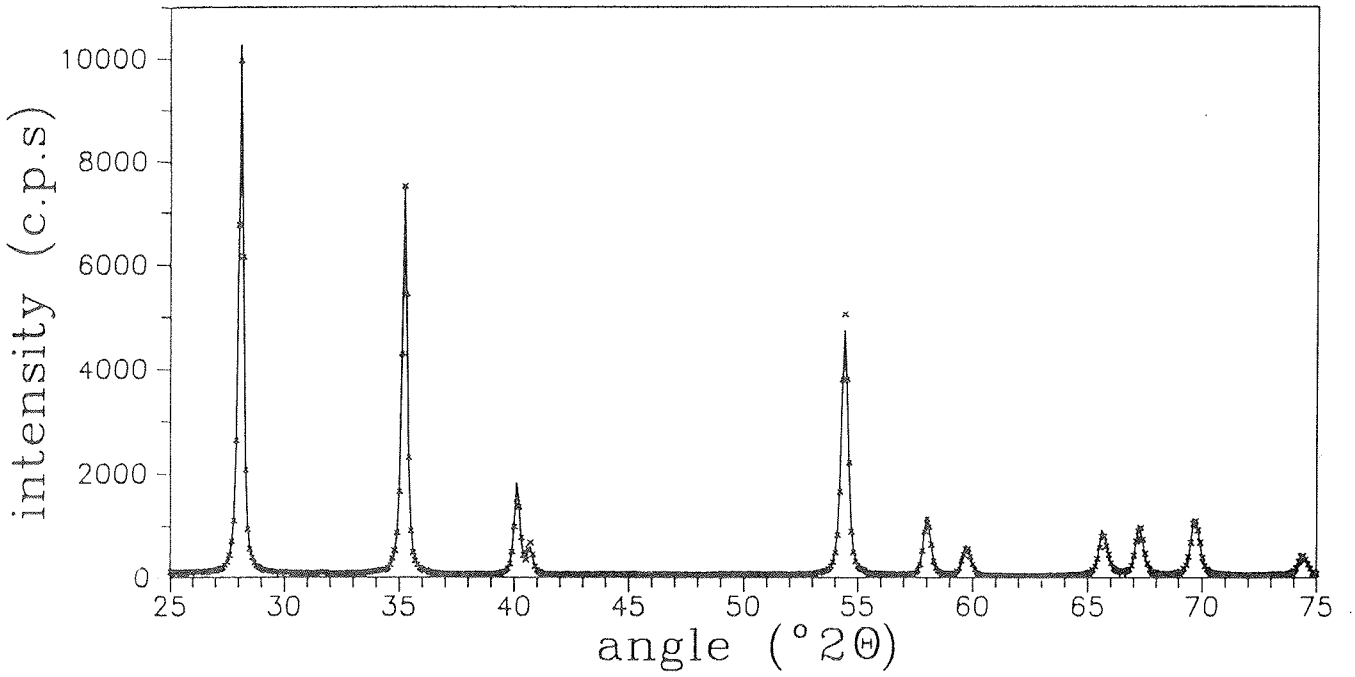


*Fig. 10 Rietveld analysis of the diffraction profile, powder of $RuO_2$*

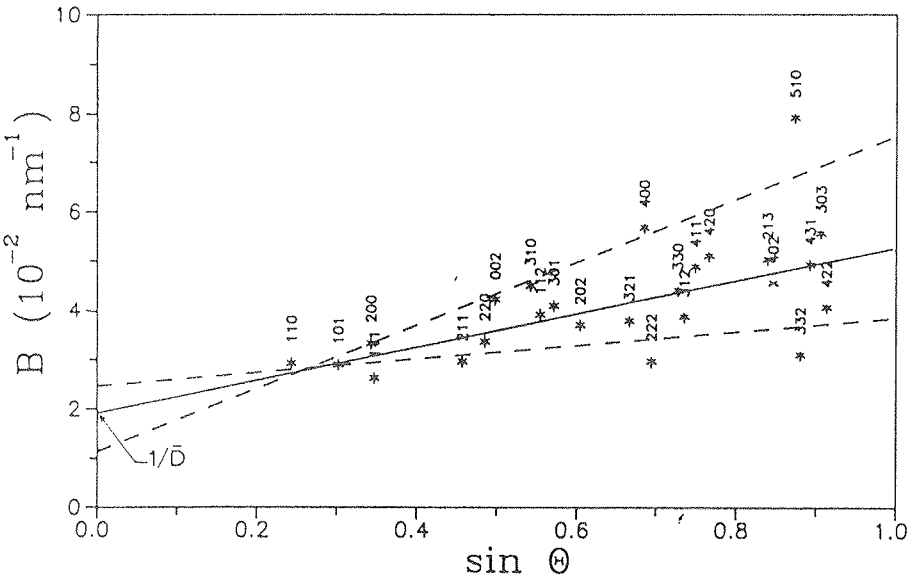


*Fig. 11 Dependence of B (hkl) vs. sin Θ*

*Tabele 1:* Structure parameters of $RuO_2$ powder, Ru-109 by Shoei Chem. Inc.

| Lattice parameters | Fractional atomic coordinates |
|---|---|
| a = b= (0.44900 ± 0.00009) nm | Ru : (0, 0, 0) |
| c = (0.30920 ± 0.00006) nm | O : (0.3034(9), 0.3034(9), 0) |

The dependence B(hkl)vs. sin Θ is shown in Figure 11, where the significant reflections are indicated. Both the strain e and the size D of $RuO_2$ coherent domain are given in Table 2. The integral breadths were calculated using the total pattern analysis. Experimental data were approximated with the Pearson VII function:

$$y = a_1 / [a_3 \cdot (x - a_2)^2 + 1]^{a_4}$$

y is the number of pulses per second, x= sin Θ.

*Table 2:* Microstructure parameters of $RuO_2$ powder, Ru-109 by Shoei Chem. Inc.

| | min | max | mean value |
|---|---|---|---|
| D | (42 ± 1) nm | (74 ± 3) nm | 53 nm |
| e | $(0.5 \pm 0.1)\times10^{-3}$ | $(2.3 \pm 0.2)\times10^{-3}$ | $1.4\times10^{-3}$ |

Other parameters:

- $a_1$ ... the height of the maximum,
- $a_2$ ... the position of the maximum,
- $a_3$ ... the parameter connected with line breadth,
- $a_4$ ... the shape parameter.

As an external standard for instrumental broadening, the tungsten carbide was used.

These analyses were carried out for several types of $RuO_2$ powders. The results and mean values of microstructure parameters are listed in Table 3. The high values of the strain e for Engelhard and Johnson-Matthey (800-2MX) powders show that these materials were probably prepared by intensive grinding contrary to Shoei Chem. Inc. and Johnson-Matthey (800-3C) powders characterized by a very low microstrain. Johnson-Matthey (800-3C) powder exhibits a very strong preferred orientation in the <110> direction.

*Table 3:* Microstructure parameters of various $RuO_2$ powders (mean values)

| Type of $RuO_2$ | D (nm) | e ($10^{-3}$) |
|---|---|---|
| Engelhard | 9 | 15 |
| Jonhson-Matthey | | |
| 800-3C | 75 | 0.5 |
| 800-2MX | 6 | 7.5 |
| Shoei Chem. Inc., Ru-109 | 53 | 1.4 |

The microphysical parameter of our $RuO_2$ microcrystalline powder compared with Shoei. Chem. Inc. are given in Table 4.

*Table 4:* Microphysical parameters of Shoei Chem. Inc. and our $RuO_2$ powders (mean value)

| | Shoei Chem. Inc. | Our production |
|---|---|---|
| a (nm) | 0.44985(± 9) | 0.45027(± 5) |
| c (nm) | 0.30975(± 5) | 0.30990(± 5) |
| D (nm) | 53 | 21 |
| e ($10^{-3}$) | 1.4 | 2.0 |
| Fractional atomic | | |
| O-coordinates | (0.3034, 0.3034,0) | (0.3034, 0.3034, 0) |

We can see that all the parameters are in very good agreement. Only the grain sizes are smaller as it is shown in Fig. 12 and Tab. 4.

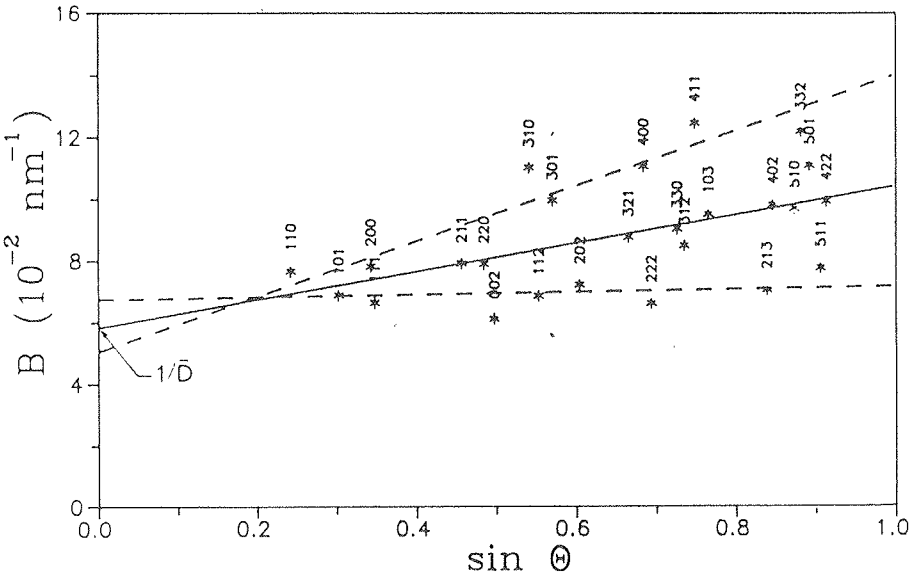


*Fig. 12 Dependence of B (hkl) vs. sin Θ, our powder $RuO_2$*

The X-ray analysis of the various $RuO_2$ powders was consistent with the microscopy investigation.

## 6. RESISTIVE THICK FILMS BASED ON NEW PASTES CONTAINING $RuO_2$

### 6.1. Resistive paste preparation

#### Glass powder

In the systems containing glass and electric conductive components the whole range of glass types of various compositions is being used as mentioned above. Based on a long experience, glass frits of the system PbO-$Bi_2O_3$-$SiO_2$-$B_2O_3$ were investigated. These glass types were prepared in various compositions. For a further larger investigation a system was chosen, containing in addition to the mentioned components, in a suitable fractional relation, also a smaller amount of CaO.

Glass powder preparation consisted in several steps:

1) pelletizing the respective oxides at the temperature of 450°C for one hour,
2) the melting process carried out at the temperature of 1450°C in a platinum-rhodium crucible for one hour with intensive mixing,
3) cooling-fritting the molten glass into water,
4) grinding the glass frit in the agate planetary ball mill Fritsch Pulverisette 5, for 50 hours.

The grain size (about 3 - 5 μm) and surface area (1.6$m^2$/g) of the powder were determined by the instruments mentioned above.

The parameters of this glass frit were as follows:

- density: 4.6 g/$cm^3$,
- thermal expansion coefficient: 7.1 x $10^{-6}$/K,
- transformation point: 480°C,
- deformation point: 530°C,
- sealing temperature: 695°C.

#### Ruthenium dioxide

Using a previous experience, ruthenium dioxide, type Ru-109 produced by Shoei Chemical Inc. was chosen as an electrical conductive component of pastes. It is characterized by its grains which are perfect small single crystals long about 53 nm (see Table 2 and Fig. 4a). The same $RuO_2$ powder (Ru-109) was used for new excellent resistive pastes R-1000N Series produced by Shoei Chem. Inc.

#### Paste mixing

Pastes were prepared by mixing the glass powder, ruthenium dioxide Ru-109 (Shoei Chem Inc.) and liquid vehicle containing terpineol and 10 wt.% ethyl cellulose. The pastes were mixed in Fritsch equipment Pulverisette 2 with an agate garniture for about 1 hour. No further ingredients were used for the paste preparation. On the whole, 28 various pastes (in two series) containing various contents of $RuO_2$, ranging from 2 vol.% to 22 vol.% were prepared. Paste viscosity (of about 180 Pa.s) was measured with the Brookfielde Digital Viscometer, Model HBT DV-II.

### 6.2. Thick film preparation

Thick film resistors were prepared by a screen-printing the pastes onto alumina substrates, to a dried film thickness of about 15 μm. Two types of alumina substrates, AlSiMag 860 and SA 305 50 (produced by Tesla Hradec Kralové) provided with AgPt terminations were used for the preparation of two types of resistor test patterns (see Fig. 13 a,b). The film dimensions (lenght

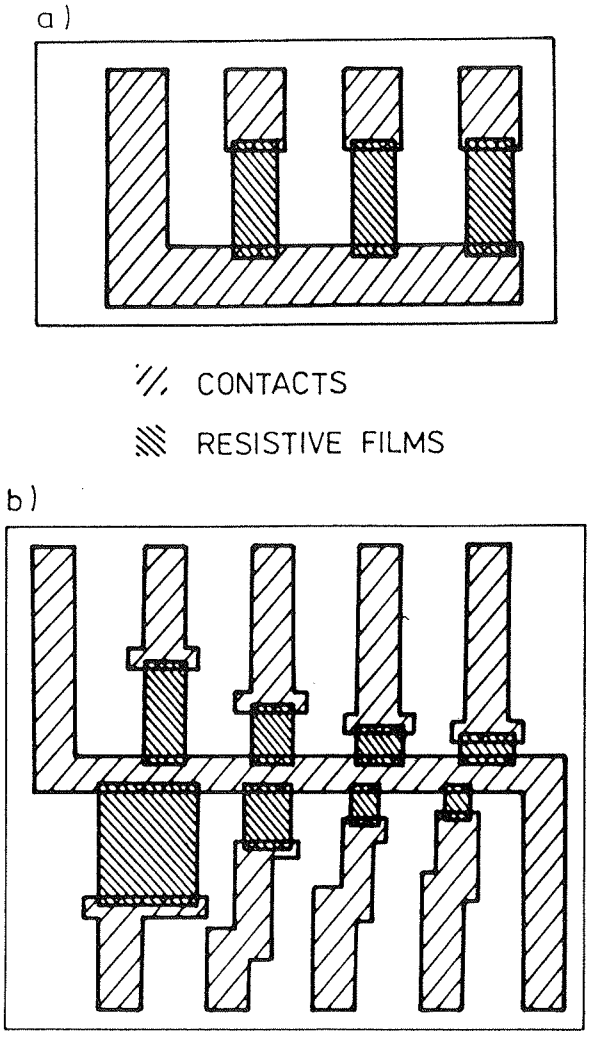


*Fig. 13a,b Two types of resistor test patterns*

and width) ranged from 1 mm to 5 mm (1x1, 1.5x1.5, 2.5x2.5, 5x5, 1x2.5, 1.5x2.5, 2.5x2.5 and 4x2 mm).

The films printed and dried at the temperature of 120°C were further fired in a furnace with a suitable temperature schedule at peak temperature of 850°C. The total firing cycle lasted over 1 hour with 12 minutes at peak temperature. Several hundreds of thick films were prepared by this method.

The surface profile, thickness, cross-section area and roughness of the films were tested by means of the Surfometer SF 200 produced by Planer Products Ltd. For illustration, there are two readings (see Fig. 14 and 15) carried out on fired resistor films containing 10 and 20 % by weight of $RuO_2$, respectively. They indicated that the film thickness was about 8-9 μm, the area reached the values of about 17,000 $\mu m^2$ and the roughness depended on the paste type, mainly on the glass contents in the paste.

## 7. BLENDING CURVES

The blending curve belongs to the basic characteristics of resistive thick films. It describes the relation between the conductive phase contents and the film resistivity.

The test pattern containing a triad of thick films 4 mm long and 2 mm wide (see Fig. 13a) was used for this investigation. The measured values of resistance should be divided by the factor 2 to obtain sheet resistance.

### 7.1. Measurement set-up

The blending curve investigation is based on measurement of a large amount of resistive thick films containing different concetration of conductive particles ($RuO_2$ in our case).

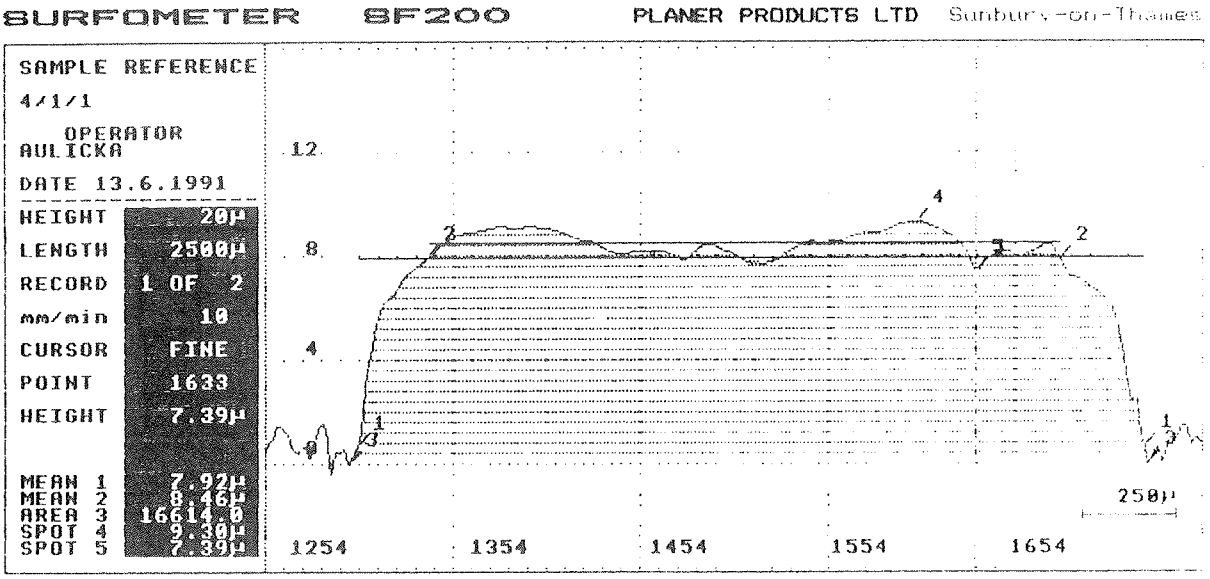


*Fig. 14 Surface analysis, fired resistor film containing 10% by weight of $RuO_2$*

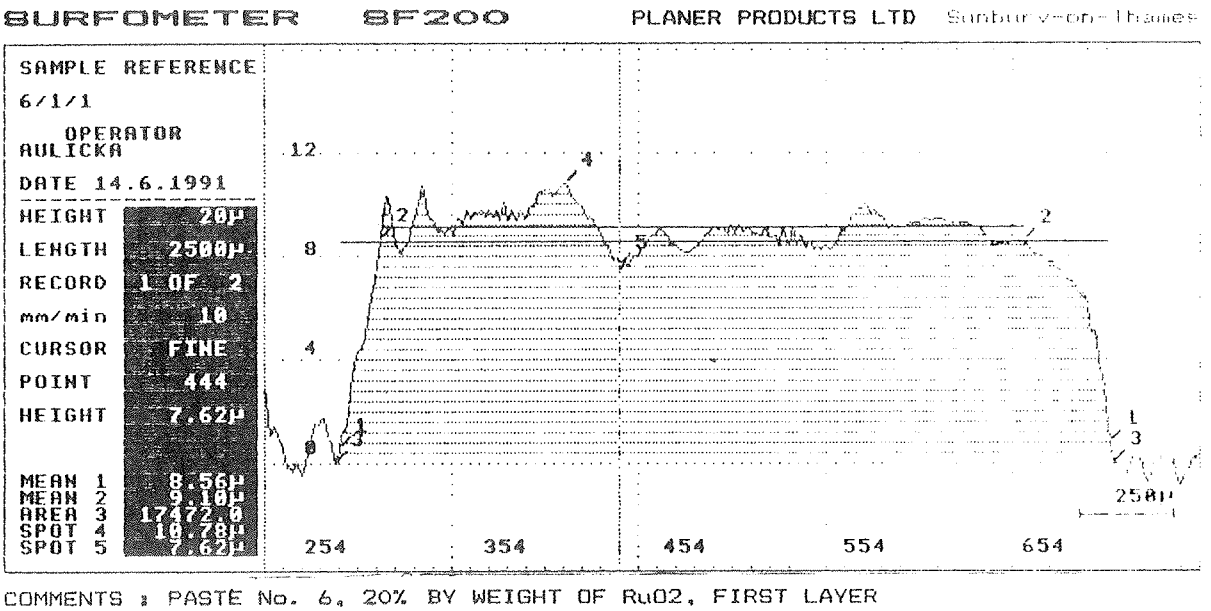


*Fig. 15 Surface analysis, fired resistor film containing 20% by weight of $RuO_2$*

The experimental set used by us for measuring the resistance of the films is shown in Fig. 16. It consists of a Source Measure Unit (SMU) Keithley K 238 and a Scanner Keithley K 705 with a measuring holder. The SMU K 238 serves as a voltage source and an ammeter simultaneously. The Scanner K 705 together with the holder gives an opportunity to measure automatically up to 36 samples at a time. Both the SMU and the Scanner are controlled via IEEE-488 bus by a PC-AT compatible computer.

An electrical schematic diagram is shown in Fig. 17. The SMU K 238 is used in a "local sense" mode. It means that 2-wire resistance measurement is performed. The holder includes 48 pin Pd-Ag terminals that serve for connecting up to 36 samples fixed on 12 alumina substrates. In order to enable to switch automatically all 36 samples, two General Purpose Scanner Cards Keithley K 7156-D in 1-pole mode are used. However, the General Purpose Cards offer no possibility to use guarding. Therefore a special attention must be paid to a parasitic capacitance and a leakage current.

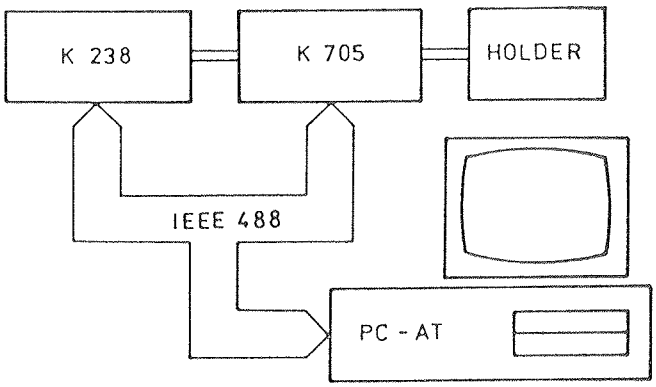


*Fig. 16 Experimental set used for measuring the resistance of the films*

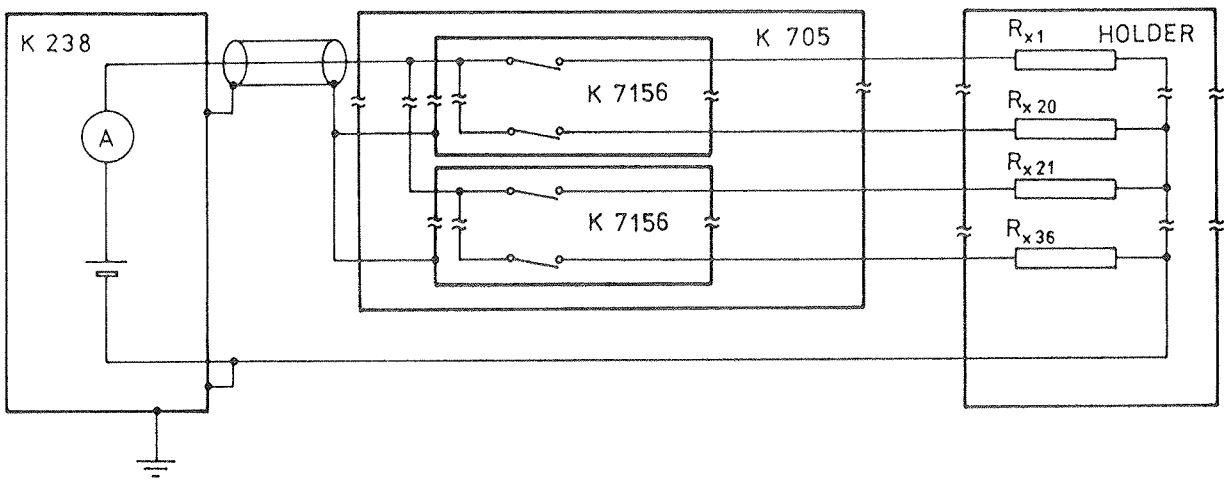


*Fig. 17 An electrical schematic diagram of the experimental set*

### 7.2. Concentration dependence of resistivity

Two series of samples were measured. The first one contained 12 thick films (on 4 substrates) for each of 11 volume contents from about 2% to about 22% of ruthenium dioxide. The second series contained also 12 resistive samples for 17 volume concentrations from about 2% to 14% (alumina substrates SA 305 50 were used only).

The results are presented in form of graphs. In Figures 18, 19 and 20 values obtained for both series are plotted. Each point in the graphs represents an average value obtained from 12 films for a given concentration in a given series. The results were not influenced by the used substrate type.The corresponding dependence plotted in a linear scale (Fig. 18) shows a strong increase of the resistivity for concetrations below 3 vol. %. This type of the dependence is usually explained by means of the percolation theory. The concentration dependence of the thick film resistivity can be compared to the dependence of the resistivity in a percolating system. The percolation theory uses the blending curve equation

$$R = R_0 (v - v_c)^s \qquad (3)$$

to describe the relation between the volume concentration v of conducting phase in a system and its resistivity R near the critical volume concetration $v_c$ at which transition insulator – resistor occurs; $R_0$ and s are the material constants.

In order to obtain the values $v_c$, s and $R_0$ from the measured dependence R versus v, the following procedure based on a weighted least-squares fit was used.

The measured values $R_{ij}$ for N samples (j from 1 to N) with the 1-th concentration have an equal statistical weight $p_i$ given byequation

$$p_i = \sigma_i^{-2} \qquad (4),$$

where dispresion $\sigma_{i\,2}$ is given by equation

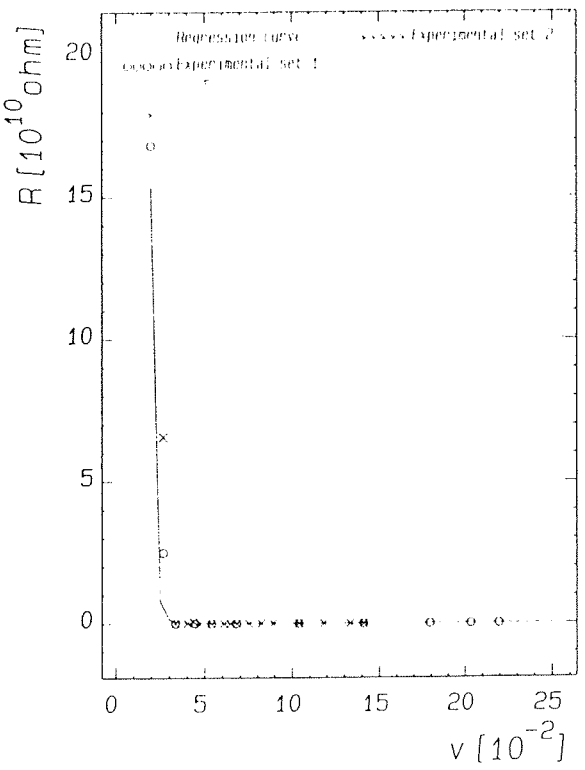


*Fig. 18 Resistance versus vol. concentration of $RuO_2$*

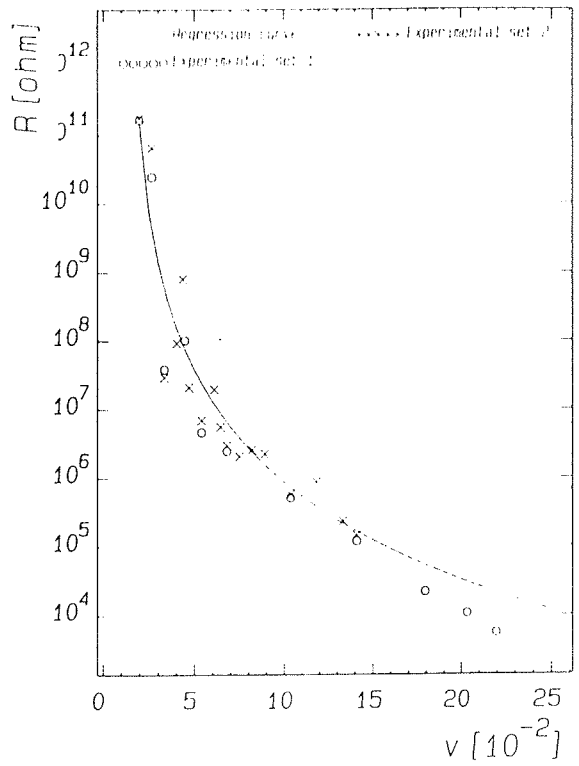


*Fig. 19 Resistance vs. vol. concentration of $RuO_2$*

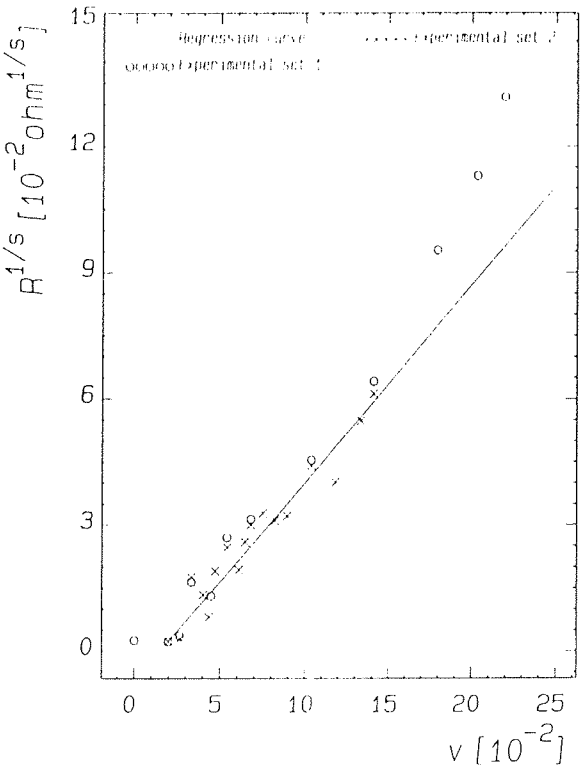


*Fig. 20 $R^{1/2}$ curve for measured data*

$$\sigma_i^2 = \frac{\sum_{j=1}^{N} R_{ij}^2 - \frac{\left(\sum_{j=1}^{N} R_{ij}\right)^2}{N}}{N-1} \qquad (5).$$

However, the function in (3) is not linear and there are three unknown constants $R_0$, $v_c$ and s present. Therefore it is suitable to find the straight lines

$$R^{1/s} = R_0^{\,1/s}\,(v - v_c) \qquad (6)$$

with two fitted parameters $R_0$ and $v_c$ for different fixed values of exponents. The best fit will be that giving the linear correlation coefficient closest to one. It must be taken into account that weight of the value $R_{ij}^{1/s}$ is given by the relation

$$p_{ij} = \frac{p_i}{\left(\frac{d\left(R_{ij}^{1/s}\right)}{dR_{ij}}\right)^2} = \frac{s^2 p_i}{\left(R_{ij}^{1/s-1}\right)^2} \qquad (7).$$

The solid lines in Figures 18, 19 and 20 represent a blending curve obtained from the least-squares fit for the second series. The fit can be considered to be very good. The unknown parameters obtained from the fit:

the critical volume $v_c = 1.5 \pm 0.1$ vol.% and

the critical exponent $s = -4.3$

It can be seen that the value of the critical volume $v_c$ is rather small in comparison with the theoretical value $v_c \cong 0.3$ predicted by the percolation theory. This fact is usually explained by the difference between the homogeneous distribution of conducting particles presumed by the theory and a real distribution of conducting particles in glass of a thick film. We suppose that the distribution essentially differs from homogeneous one and some kind of segregated structure containing complete conductive chains is formed especially at low concentrations. The merit of such distribution consists in the fact that we can obtain resistive films with low resistivity for relatively low concentration of conductive particles.

## 8. VOLTAGE AND TEMPERATURE DEPENDENCES OF RESISTIVITY

Dependences of resistivity on temperature and electric field were measured for the thick films containing various contents of $RuO_2$ powder. The respective experimental set-up was arranged for this purpose.

### 8.1. Measurement set-up

The experimental arrangement for measuring the resistance vs. voltage dependence and the resistance vs. temperature dependence is illustrated in Fig. 21. K 237 is the Keithley High Voltage SMU (Source Measured Unit) used for both supplying voltage and measuring current, K 706 is the Keithley Scanner mainframe used for switching signals to a particular resistor, VLK 07/90 is the Labotest Humidity Chamber produced by Heraeus - Vötsch which is used for setting and stabilizing temperature and humidity, VRSU is the interface to the Labotest Humidity Chamber. All devices are connected through the IEEE-488 (GPIB) bus and they are controlled by the PC/AT compatible computer.

An electrical schematic diagram is shown in Fig. 22. In order to decrease time consumption the scanner switsching is employed and it is possible to measure 8 resistors on the same substrate at once. The high voltage SMU is switched to a "local sensing" mode (the "remote sensing" mode means the four-terminal connection necessary for low resistance samples only) and only coaxial cables are used for low wiring. K 7154 is a Keithley High Voltage Scanner Card. According to specifications of this card and assuming other possible error sources (leakage currents, capacitances etc.), we have found coaxial cables to be convenient enough for these purposes. The alumina substrate with printed resistors (thick-film) is mounted to a teflon holder and wires are soldered to the terminals. The whole holder is placed into the Labotest Humidity Chamber which guarantees both the temperature stability and electrical shielding.

The SMU is able to supply voltage as high as 1100 V and to measure current as low as 10 fA. The voltage drop across the ammeter is less than 1 mV. Using a logarithmic pulsed sweep of voltages appears to be the most adequate measure for our task. It allows characterization over several decades of voltage and prevents an increase of temperature of the sample during measurement due to Joule's heat at the same time (Fig. 23).

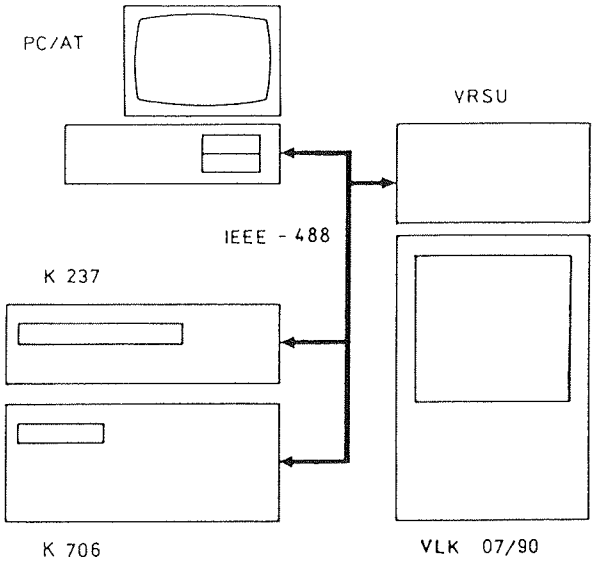


*Fig. 21* *The experimental arrangement for measuring the resistance vs. voltage*

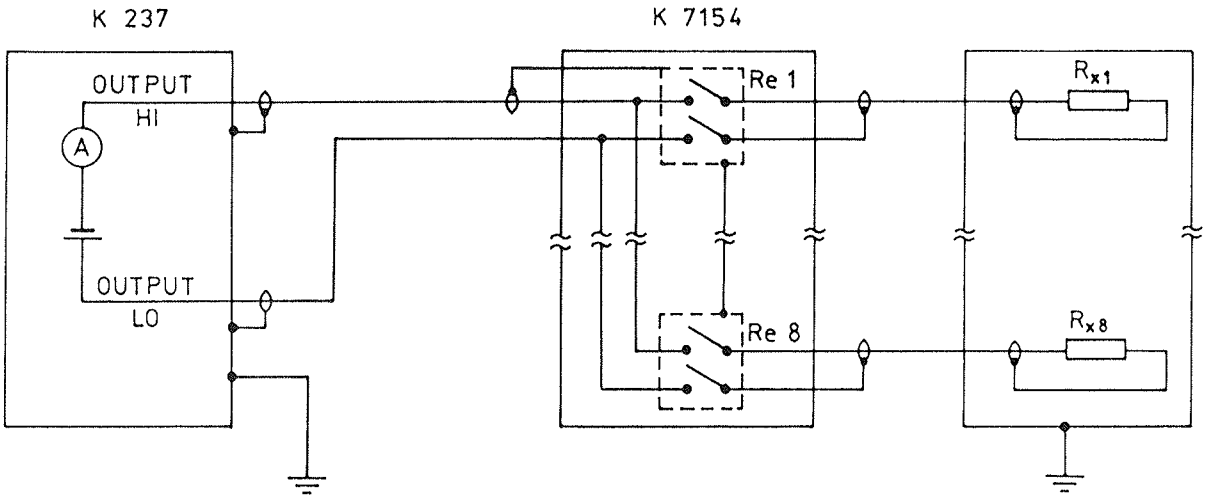


*Fig. 22* *An electrical schematic diagram of the experimental arrangement*

$t_{ON}$ – "time on" parameter is used as short as posible but some delay must be included for establishing required voltage ($t_{ON}>10\tau$, where $\tau$ = RC is the relaxation time when parasitic capacitances are taken into account). A measure phase is performed at the end the voltage pulse. $t_{OFF}$ – "time off" parameter is chosen several times larger than time on to allow a sufficient heat transfer from the sample to the surroundings.

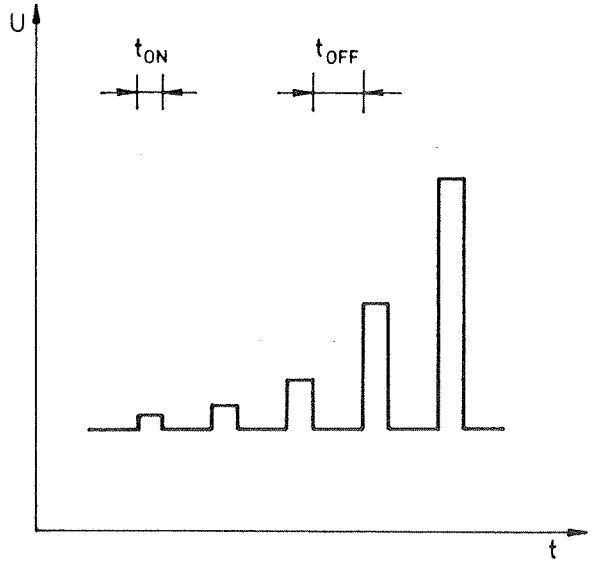


*Fig. 23 Shape of logarithmic pulsed sweep of voltages used for measurements*

### 8.2. Resistivity versus voltage measurements

The aim of this measurement is to characterize the changes in resistence value over a wide range of the electric field applied.

The electric field starts from the value less than 0.1 V/mm and stretches up to the value 400 V/mm, permitting voltage source and current compliance. Parameters $t_{ON}$ and $t_{OFF}$ are selected with great care for each set of resistors. The measurement is carried out at the tempreature 22°C which is stabilized by the Labotest Humidity Chamber.

For illustration, there are only some results presented in the forms of graphs (Figs. 24, 25, 26) for resistors prepared using three pastes containing $RuO_2$ in contents of 5.4, 3.34 and 2.66 vol. %, respectively. Relative changes in the resistance value are plotted versus the electric field E for various resistor dimensions. The resistance value obtained at the electric field of 0.1 V/mm is assumed as a reference value and the relative change is calculated according to the formula

$$\delta R = \frac{R_{meas} - R_{0.1}}{R_{0.1}} = \frac{\Delta R}{R_{0.1}} \qquad (8)$$

A logarithmic scale is used in the voltage axis for a better orientation in the graph.

Generally, we can distinguish two regions in the R-E characteristics. The first region is a plateau - the value of resistance remains almost unchanged over a wide range (for $R<10^7$ Ω/sq.) of applied voltage. The refer-

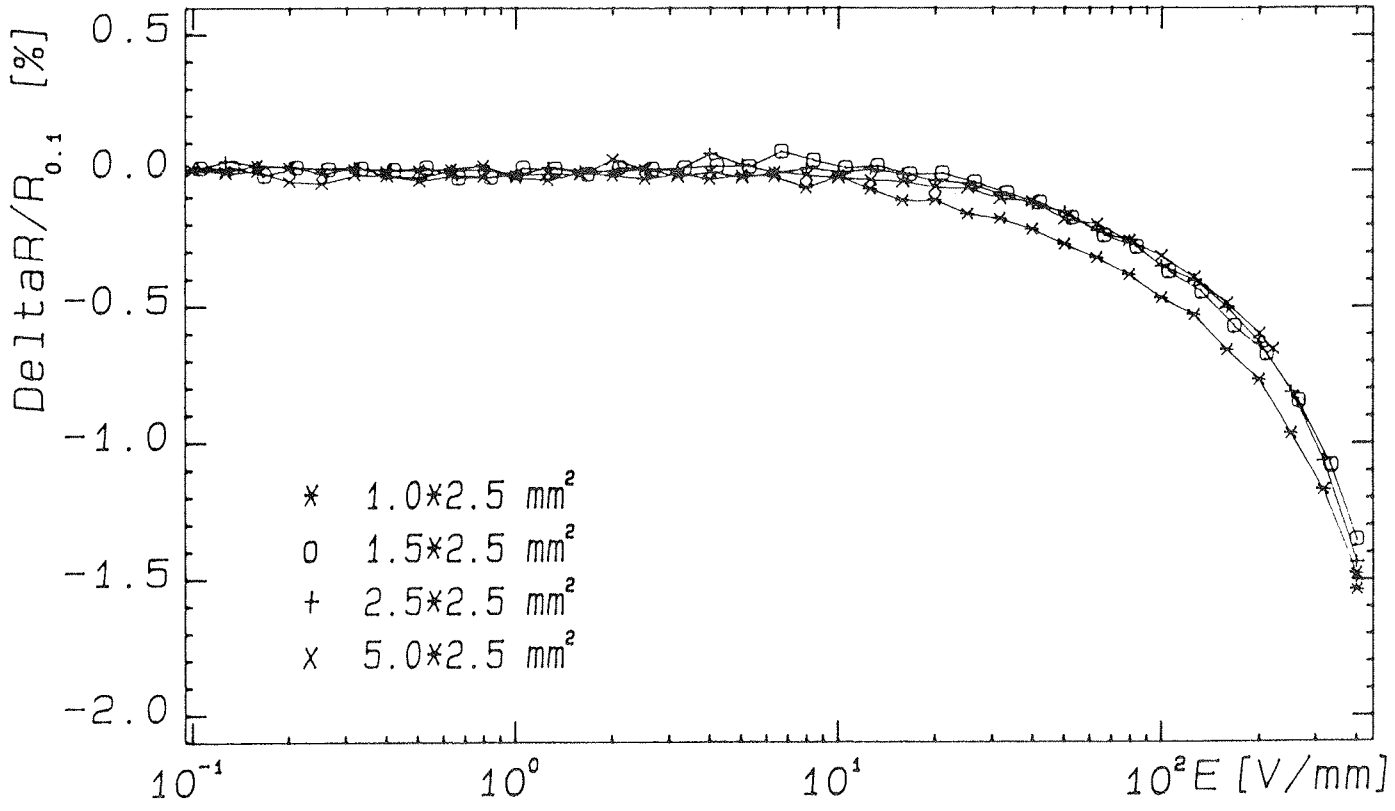


*Fig. 24 Relative change in the resistance value vs. electric field for various resistor dimensions, 5.4 vol % $RuO_2$*

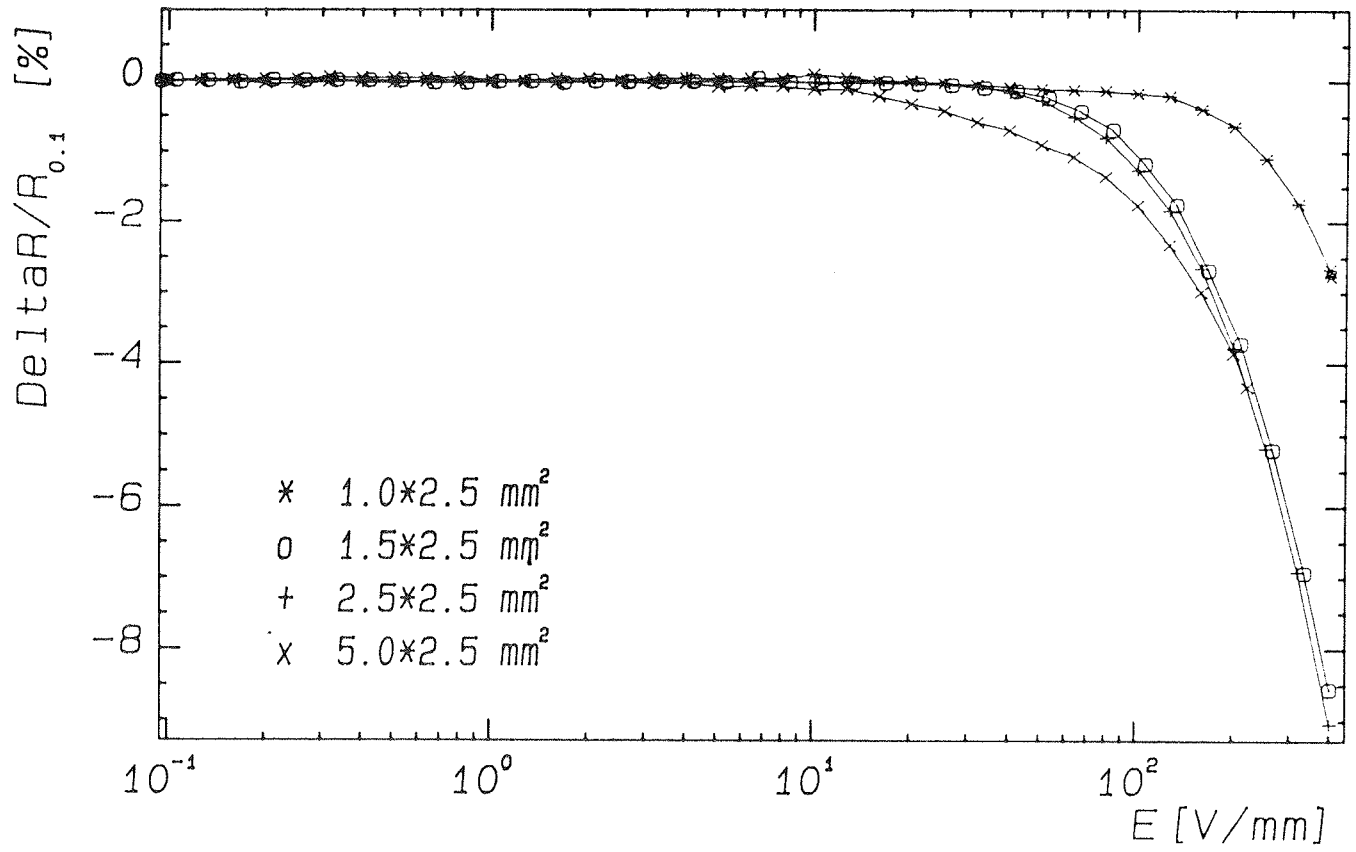


*Fig. 25 Relative change in the resistance value vs. electric field for various resistor dimensions, 3.34 vol % $RuO_2$*

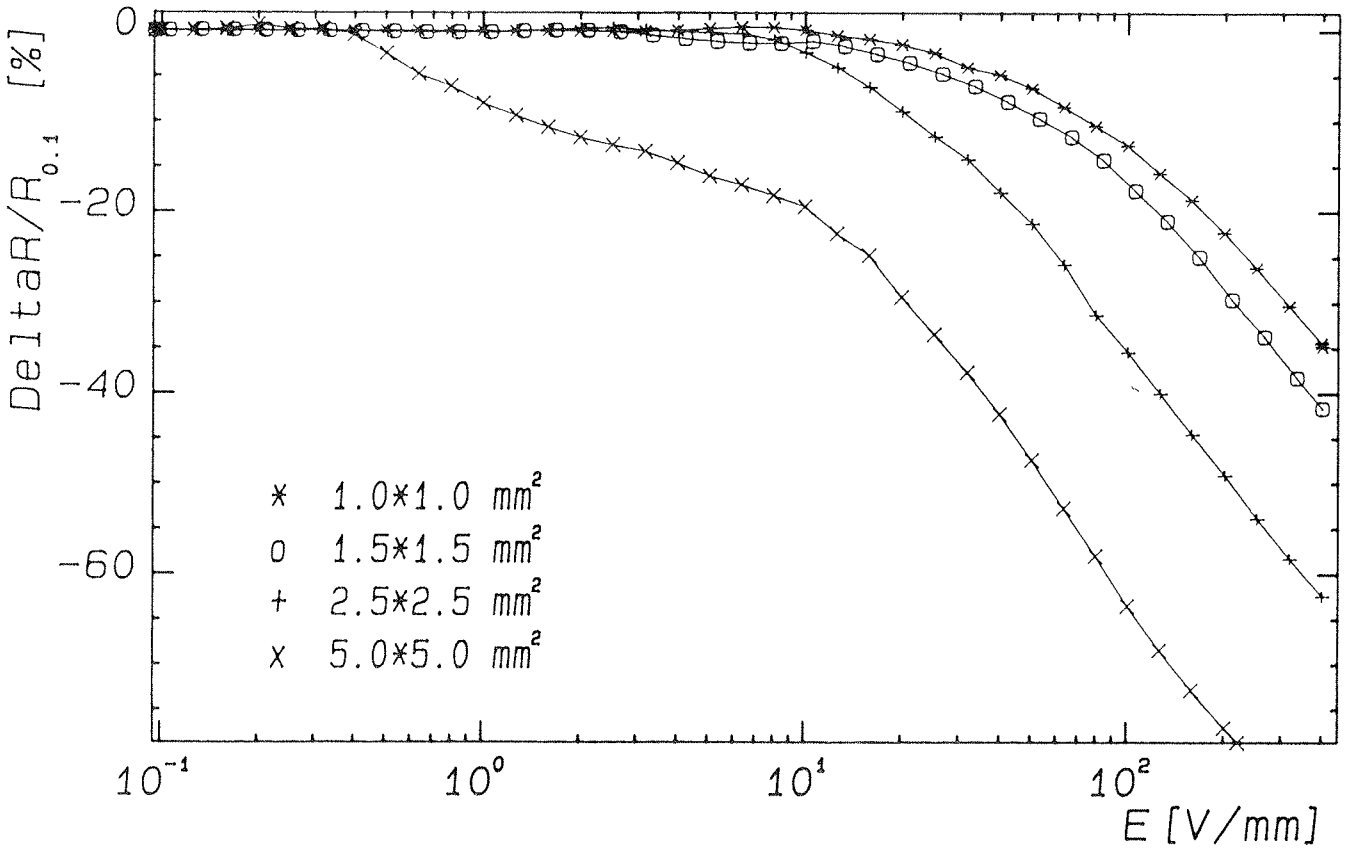


*Fig. 26 Relative change in the resistance value vs. electric field for various resistor dimensions, 2.66 vol % $RuO_2$*

ence value, E = 0.1 V/mm, belongs to this region. A different choice of the reference value does not affect the results if it lies within the plateau region. In the second region a relatively sudden decrease in resistence occurs. The position of the boundary between the plateau and the decline region depends slightly on the resistive paste and sheet resistivity (see Figs. 24 - 26). The voltage limit (1100V) or the current limit (100 mA on 110 V range and 10 mA on 1100 V range) of the SMU do not allow to reach the electric field of 400 V/mm for every resistor.

No substantial difference between two substrate types was found. The slope of the characteristics in the decline region is strongly dependent on the sheet resistance. Low resistivity films exhibit a relative change in resistance which does not exceed a few tenths of per cent for 200 V/mm (about 0.7% for $1.3 \times 10^6$ Ω/sq, see Fig. 24), while those of high resistivity exert a change in relative resistance of several tens of per cent for 400 V/mm (Fig. 26). Resistance depends very slightly on voltage for electric field up to 50 V/mm until sheet resistance of the sample does not exceed the value of obout $5 \times 10^6$ Ω/sq, the same for different lengths of film. The voltage coefficient of resistance is usually about 30 ppm/V/mm or less in the plateau region. For high resistive samples ($R > 5 \times 10^6$ Ω/sq.) the plateau width depends on the length of a resistor (see Figs. 25 and 26).

A greater difference among particular resistors was observed for some samples, usually those with higher resistivity ($R > 10^7$ Ω/sq.). The "breakdown electric field" denotes the field of the transient from the plateau into the region with decreasing resistance. The term does not mean real breakdown. Both the "breakdown voltage" and the slope of the characteristics in the decline region are subjected to changes. The correlation between the "breakdown voltage" value and dimensions of the resistor seems to be weak for sheet resistance lower than about $10^7$ Ω/sq but it is important for high resistivity films.

The shape of R-E characteristics can be described with the help of two mechanisms of charge transport. One of them provides a conductivity independent or weakly dependent on the electric field, while the conductivity connected with the other mechanism strongly increases with the electric field. The first one can be captured using traditional theories for this type of materials. It dominates in the plateau region. The other mechanism prevails in the decline region. The latter one may be connected with the Frank-Poole effect, the thermal ionization of captured charge carriers assisted by the electric field which significantly decreases the effective potential well height. A typical feature for this effect is a strong dependence on the electric field. Of course, the influence of the second type of transport is much weaker for resistors with a lower sheet resistance.

This hypothesis can explain the fact that the shortest resistors (1 mm) usually exhibit a higher "breakdown voltage". This is due to the fact that the diffusion of silver exerts an influence to a relatively larger part of the resistor. The greater the length of a resistor, the lower "breakdown voltage" it should show according to the above idea. This fact is demonstrated by Figs. 25 and 26. On the other hand, the diffusion is a rather complex phenomenon influenced by many more or less predictable factors. That is why, the prediction does not hold in every case.

The thick film resistors significantly differ in their length from the resistors used for high voltage purposes. That is why the influence of the diffusion of silver from terminals is negligible in real resistors. Anyway, the resistors in study can be used for high voltage purposes. When designing the resistors, the required specifications (dimensions, resistivity value and its change, working voltage, etc.) must be taken into account.

The results presented suggest the necessity of adding an another conductive component into the paste (besides $RuO_2$) in order to accomplish a wider plateau region for high resistance samples.

### 8.3. Resistivity versus temperature measurements

The temperature stability is one of the most important parameters of commercial resistors. That is why the temperature dependence of resistivity has been measured over the temperature range – 60°C to 130°C. The temperature step 5°C is assumed to provide a sufficient resolution. The resistance measurement is carried out at the electric field of 2 V/mm which is a value high enough to provide supplying voltage with good resolution and accuracy and on the other hand low enough so that it belongs to the range with a very weak field dependence of resistivity. The actual temperature can differ from that set 1°C at maximum.

Similarly to the resistance vs. voltage dependence the relative change in resistance is given by

$$\delta R = \frac{R_{meas} - R_{25}}{R_{25}} = \frac{\Delta R}{R_{25}} \qquad (9).$$

This is plotted versus the temperature. The resistance value at the temperature 25°C is assumed as a reference one and both hot (H-TCR) and cold (C-TCR) temperature coefficient of resistance refer to the following value:

$$\text{H–TCR} = \frac{R_{125} - R_{25}}{R_{25}} \cdot \frac{10^6}{100} \text{ (ppm/K)}, \qquad (10)$$

$$\text{C–TCR} = \frac{R_{125} - R_{-55}}{R_{25}} \cdot \frac{10^6}{80} \text{ (ppm/K)}. \qquad (11)$$

These two coefficients are widely used for the characterization of thick film resistors.

There are only some results presented in the form of graphs (Figs. 27 - 29) in a very similar manner to that of R-E measurements.

The curves have a concave shape with a flat minimum the position of which depends on the resistance value of samples (i.e. on the paste used). Samples with lower sheet resistance (<$5x10^3$ Ω/sq.) exhibit the minimum below the room temperature (see Fig. 27) while for that with higher resistance the minimum shifts towards higher temperatures (see Figs. 28 and 29). The observed data can be described using the second order polynomial, at least within the limited interval. This is a very common result in thick film resistor studies.

The temperature coefficient of resistance is relatively small in the absolute value. The sign of it is given by the position of minimum of each curve. The values of cold TCR, hot TCR as well as sheet resistance can be seen in Table 5 for some samples. They are the mean values of all eight resistors of each sample.

Table 5: Summary of C-TCR and H-TCR

| Sample | v | R | C-CTR | H-TCR |
|---|---|---|---|---|
| | (vol.%) | (*/sq.) | (ppm/K) | (ppm/K) |
| 1/1 | 3.34 | $1.2x10^7$ | -185 | -140 |
| 1/1SA | 3.34 | $1.2x10^7$ | -187 | -132 |
| 2/1 | 4.48 | $1.1x10^7$ | -215 | -120 |
| 2/1SA | 4.48 | $1.6x10^7$ | -235 | -118 |
| 3/1 | 5.40 | $2.6x10^6$ | -232 | -141 |
| 3/1SA | 5.40 | $2.3x10^6$ | -223 | -150 |
| 4/1 | 6.80 | $9.4x10^5$ | -206 | -138 |
| 4/1SA | 6.80 | $9.6x10^5$ | -204 | -153 |
| 5/1 | 10.38 | $2.1x10^5$ | -192 | -127 |
| 5/1SA | 10.38 | $2.4x10^5$ | -208 | -139 |
| 6/1 | 14.09 | $5.5x10^4$ | -165 | -107 |
| 6/1SA | 14.09 | $6.8x10^4$ | -175 | -116 |
| 7/1 | 17.95 | $1.3x10^4$ | -88 | -26 |
| 7/1SA | 17.95 | $1.6x10^4$ | -104 | -53 |
| 9/1 | 20.33 | $4.7x10^3$ | -5 | +45 |

When we compare the results of TCRs for both substrate types, the samples marked with SA (produced by Tesla) seem to exhibit a little greater TCRs but the difference is not very significant (see Table 5).

Both TCRs are mostly negative because the resistance usually decreases with the increasing temperature as shown in Figs. 28 and 29. The dependence of TCR (either of them) upon the sheet resistance exhibit a minimal value that is accomplished for samples 3/1 (R≒$2.5x10^6$ Ω/sq., see Fig. 30). The increase of TCR (decrease in the absolute value) towards higher sheet rasistances is weak (up to R ≒ $10^7$ Ω/sq.), while there is a significant change towards lower resistances. For samle 9/1 (R ≒$4.5x10^3$ Ω/sq.) value of H-TCR reaches a positive sign and value of C-TCR is nearly zero.

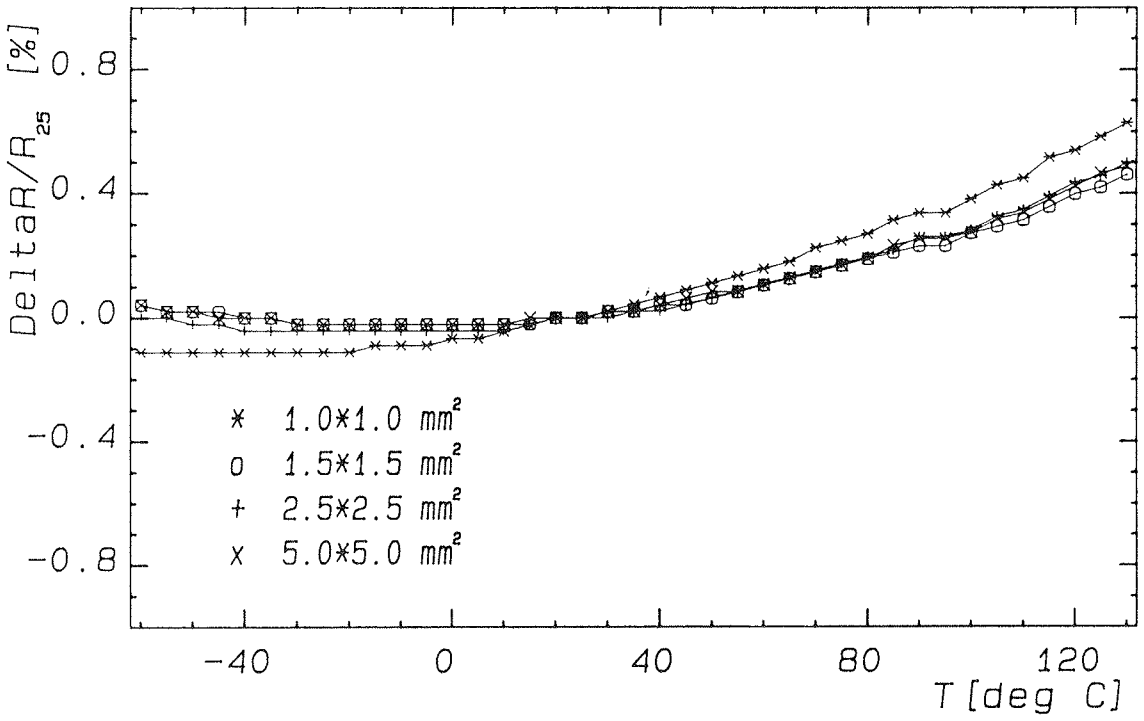


*Fig. 27 Relative change in resistance vs. temperature*

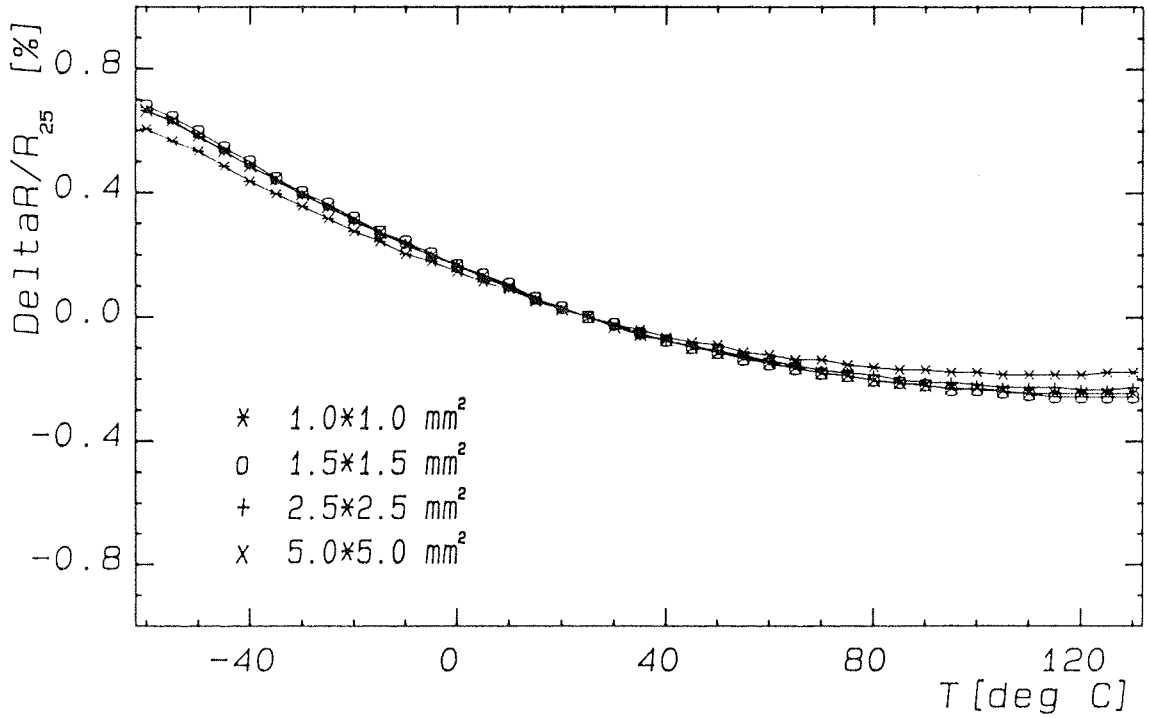


*Fig. 28 Relative change in resistance vs. temperature*

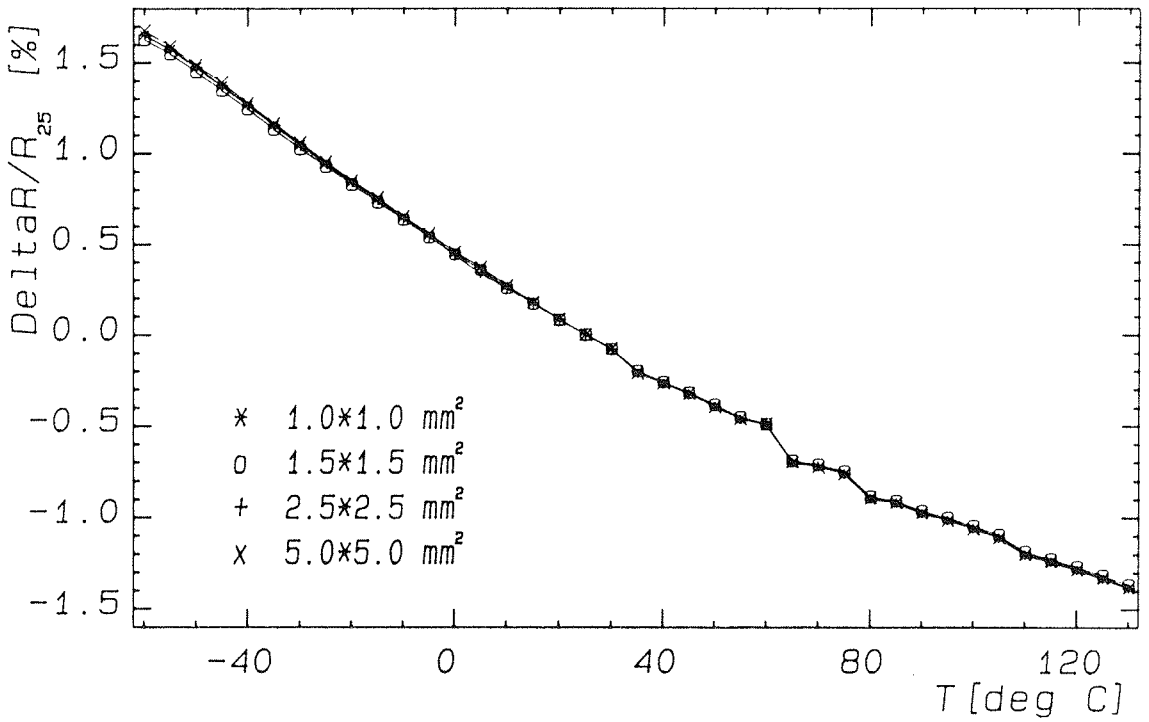


*Fig. 29 Relative change in resistance vs. temperature*

The weak dependence of TCRs on the sheet resistance for samples with resistance greater than about $10^5$ Ω/sq. is important for preaparing the resistors with high resistance and relatively low TCR. The fact that TCR is nearly independent of the thick film dimensions is of great importance as well. Some deviations can be observed for the resistors 1 mm long (see Figs. 28 and 29).

We suggest to find the physical reason in the diffusion of silver. The source of it is the conductive paste used for terminal preparation. The particles of silver can change the physical reality in the part of the sample volume, that is why the differences among particular resistors are not surprising. The dependence of resistance upon the temperature is weak especially when no additional component was used for compensating the temperature dependence of conductivity caused by $RuO_2$. An influence of diffusion of silver was observed but in real resistors this is a factor of negligible importance.

## 9. CONCLUSION

The main problems connected with the resistive paste prepararion were discussed in the paper.On one side it was shown how to solve various important tasks, and on the other hand what tecnology and measurement set-up had to be used for this purpose. Several testing methods were employed to study the problem. It was confirmed that it was very important to find the most suitable conductive solid ingredients for the pastes. Very good results were obtained with runthenium dioxide powder with particles (grains) formed by small perfect single crystals. The reaction between glasss and grains was not very important in this case and the resistive paste showed very good properties.

We can emphasize that we showed teh most important problems only. There are further tasks to be solved. It is a long-term stability of resistance in both dry and wet air at elevated temperature, for example. The latter exhibited very satisfactory results for our thick films and the resistance changes varied in tenths of per cent under the conditions of 40°C, relative humidity of 90% for 1,000 hours. Furthermore, there is a resistance change at the electric power and similarly. All these data are usually given in the information brochure on properties of respective thick film resistors.

We also started to study the admitance of resistive thick films in sandwich structure for various temperatures and frequencies. The results will be presented after the experiment finishing in the near future.

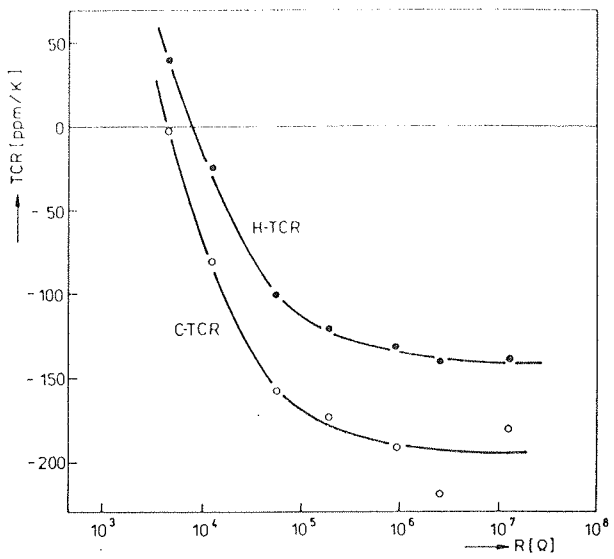


*Fig. 30 TCR vs. resistance*

## References

(1) H. Saito, M. Yamazoe, S. Matsumura, N. Yoshiha: Proc. 8th European Hybrid Microelectonics Conference. Rotterdam. May 28-31 1991, 385.

(2) R. Kužel, M. Hrovat, M. Pristavec, J. Pešička, P. Osif:

Zbornik referatov XXVI. Jugoslovanskega simpozija o elektronskih sestavnih delih in materialih SD90, Radenci 19-21. September 1990, 235.

(3) D.B. Wiles, R.A. Young: J. Appl. Cryst. 14, 149 (1981).

(4) C.N.J. Wagner, E.N. Aqua: Advanc. X-ray Anal. 7, 46-65 (1963).

(5) V. Valvoda, R. Černy, R. Kužel, L. Dobiášová: Cryst. Res. Technol. 22, 1301-1311 (1987).

*Prof. Radomir Kužel*

*RNDr. Ivo Křivka*

*RNDr. Oto Stefan*

*RNDr. David Rafaja*

*Ph.D. Josef Pešička*

*RNDr. Jan Prokeš*
*Faculty of Mathematics and Physics*
*Charles University*
*Ke Karlovu 5*
*121 16 Prague 2, Czechoslovakia*

*Prof. Josef Kubát*
*Depertment of Polymeric Materials*
*Chalmers University of Technology*
*S-412 96 Gothenburg, Sweden*

*Marko Hrovat, Dipl. Ing.*
*Jožef Stefan Institute*
*Ljubljana University*
*Jamova 39*
*61111 Ljubljana, Slovenia*

*Ing. Josef Broukal*
*State Glass Research Institute*
*Škroupova 957*
*501 92 Hradec Králové, Chechoslovakia*